Effects of the twin-arginine translocase on secretion of virulence factors, stress response, and pathogenesis

Urs A. Ochsner, Aleksandra Snyder, Adriana I. Vasil, and Michael L. Vasil*

Department of Microbiology, University of Colorado Health Sciences Center, Campus Box B-175, 4200 East Ninth Avenue, Denver, CO 80262

Communicated by Roy Curtiss, Washington University, St. Louis, MO, April 19, 2002 (received for review February 25, 2002)

A novel secretion pathway originally found in plants has recently been discovered in bacteria and termed TAT, for "twin-arginine translocation," with respect to the presence of an Arg-Arg motif in the signal sequence of TAT-secreted products. However, it is unknown whether the TAT system contributes in any way to virulence through the secretion of factors associated with pathogenesis or stress response. We found that the opportunistic pathogen *Pseudomonas aeruginosa* produces several virulence factors that depend on the TAT system for proper export to the periplasm, outer membrane, or extracellular milieu. We identified at least 18 TAT substrates of *P. aeruginosa* and characterized the pleiotropic phenotypes of a *tatC* deletion mutant. The TAT system proved essential for the export of phospholipases, proteins involved in pyoverdine-mediated iron-uptake, anaerobic respiration, osmotic stress defense, motility, and biofilm formation. Because all these traits have been associated with virulence, we studied the role of TAT in a rat lung model. A *tatC* mutant did not cause the typical multifocal pulmonary abscesses and did not evoke a heavy inflammatory host response compared with wild type, indicating that *tatC* mutant cells are attenuated for virulence. Because the TAT apparatus is well conserved among important bacterial pathogens yet absent in mammalian cells, it represents a potential target for novel antimicrobial compounds.

Secretion of proteins is a vital function of eukaryotes and prokaryotes. The general secretory pathway (Sec) has long been thought to be the only means by which proteins could traverse the cytoplasmic membrane (1). Toxins are further exported by the extracellular protein (Xcp) secretion apparatus (2) and are frequently scrutinized for their role in host–pathogen interactions (3). Sec-secreted proteins have an N-terminal sequence (i.e., secretion signal), which includes a positively charged N terminus, a hydrophobic core, and a peptidase cleavage site (e.g., Ala-X-Ala) (1).

Less than a decade ago, several investigative groups identified a novel Sec-independent secretion system that is able to secrete proteins from the cytoplasm of plants into the thylakoid spaces of chloroplasts (4, 5). This system does not depend on the hydrolysis of ATP; instead, it is driven by proton concentration differences (ΔpH) across the thylakoid membrane (6). Subsequently, in 1997 Settles *et al.* (7) reported the identification of a specific chloroplast membrane protein (Hcf106) required for the Sec-independent secretion of proteins into plant thylakoids, and interestingly, they found that Hcf106 is closely related to a bacterial protein. Further exploration of these findings by several research groups revealed that the Sec-independent protein secretion apparatus in plants is structurally and functionally very closely related to a Sec-independent, ATP-independent secretion system found in an increasing diverse array of bacterial genera.

The most noteworthy feature of the Sec-independent pathway is the nearly invariable presence of two consecutive Arg residues (TAT, twin-arginine translocation) just before the hydrophobic core (h-region) and several additional residues between the h-region and the peptidase cleavage site in the signal sequence of proteins using this pathway. Also, the N terminus of a TAT secretion signal is usually more highly positively charged than the Sec counterpart. These characteristics result in an increase in the average length of the TAT secretion signal peptide by 14 amino acids in comparison to the Sec secretion signal peptide. Yet another difference between the Sec and the TAT systems is that this novel system is capable of secreting proteins that are already folded before they enter the pore apparatus in the inner membrane (4, 5). Notably, in some cases, the TAT secretory apparatus can translocate heteromeric proteins composed of one subunit with TAT secretion signal peptide and another with no signal peptide, in a piggyback fashion across the cytoplasmic membrane. TAT-deficient mutants of *Escherichia coli* have pleiotropic phenotypes including a filamentous cell morphology, hypersensitivity to hydrophobic drugs, and characteristics consistent with an outer membrane defect (8).

A limited number of TAT-secreted proteins have been examined and they are mostly periplasmic enzymes taking part in complex, multiprotein oxidation-reduction systems involved in respiration or anaerobic growth (4, 9). Before they are secreted, TAT-dependent proteins are folded in the cytoplasm and many bind one of several redox cofactors including FeS, molybdopterin, or NiFe centers (4). Moreover, many of these cofactored proteins ultimately associate in the periplasm with other proteins of similar function that were secreted via the Sec pathway. Consequently, it would not seem that proteins secreted via the TAT system have a chance to directly interact with eukaryotic cells in a host–pathogen confrontation. Yet recently, Voulhoux *et al.* (10) showed that the secretion of two extracellular virulence determinants (phospholipase C) of the opportunistic pathogen *Pseudomonas aeruginosa* depends on the TAT secretion system. This was the first report of a protein secreted through the inner membrane by the TAT system that could be translocated further by the Xcp secretory apparatus, which is required for the secretion of many extracellular proteins (e.g., toxins) through the outer membrane.

In this report we describe several remarkable phenotypes of *P. aeruginosa* that are a consequence of the deletion of the gene encoding the TAT pore apparatus (TatC). Furthermore, we demonstrate that the secretion of proteins via the TAT system is crucial to the virulence of this opportunistic pathogen in a chronic pulmonary infection model. There are compelling reasons to believe that the TAT secretory apparatus would be a target for the development of novel antimicrobial agents.

Materials and Methods

Growth Conditions and Phenotypic Assays. The phospholipase overexpression system, methods for concentrating supernatants, and assays using the synthetic substrate nitrophenyl-phosphatidylcholine (NPPC) or Western blot analysis using a polyclonal α-PlcH Ab have been described (11). The strains harboring plasmid-borne copies of wild-type *plcHR* or mutated *plcHR*-R9K were grown for 5 h at 37°C in brain–heart infusion, transferred into M9 (1 h, 32°C), induced for 2 h with 1 mM IPTG, and normalized supernatants

Abbreviations: TAT, twin-arginine translocation; EDDHA, ethylenediamine di(o-hydroxy)phenylacetic acid; NPPC, nitrophenyl-phosphatidylcholine.

*To whom reprint requests should be addressed. E-mail: mike.vasil@uchsc.edu.

 www.pnas.org/cgi/doi/10.1073/pnas.082238299

Table 1. *P. aeruginosa* genes encoding proteins that are secreted by the TAT apparatus

Function	Encoded protein	Cellular location	Signal sequence*	Homologs in other bacteria†
Phospholipases				
plcH	Phospholipase C	Extracellular	MTENWKFRRRTFLKHGAQAATLAGLSGLFPETLRRALA	*M. tuberculosis,*
plcN	Phospholipase C	Extracellular	MISKSRRSFIRLAAGTVGATVATSMLPSSIQAALA	*Burkholderia cepacia, B. pseudomallei*
Iron acquisition				
fpvA	Ferripyoverdine receptor	Outer membrane	MPAPHGLSPLSKAFLMRRAFQRRILPHSLAMALSLPLAGYVQA	*M. tuberculosis*
PA2394	Pyoverdine biosynthesis	Periplasmic	MNDRRTFLKQAGILAAGLPLLSAAQSLRAEG	*Pseudomonas putida, P. syringae*
PA2389	Pyoverdine biosynthesis	Periplasmic	MRRTRSTRRALLVAVCLSPLIALA	
PA2392	Pyoverdine biosynthesis	Periplasmic	MTVSRRGFMAGLALTGAAALPVAYY	
Anaerobic growth				
napA	Nitrate reductase	Periplasmic	MNLTRREFAKANAAAIAAAAAGLPILVRASNLVTEADV	*Bordetella parapertussis, Yersinia*
napF	Ferredoxin	Periplasmic	MSSRRELFRRLGGHPPTRRPPWTAADFAAG	*enterocolitica, Vibrio cholerae,*
nosZ	Nitrous oxide reductase	Periplasmic	MSDDTKSPHEETHGLNRRGFLGASALTGAAALVGASA	*Salmonella enterica serovar Typhi, E. coli, Haemophilus ducreyi*
Catabolism				
fdnG	Formate dehydrogenase		MDMNRRQFFKVCGIGLGGSSLAALGMAPTEAFA	*S. enterica serovar Typhi,*
PA2124	Dehydrogenase	Periplasmic?	MHQPENPARRTLLAQTVAGSAALALGSLLGGAPGVASA	*E. coli*
PA2264	Dehydrogenase	Periplasmic?	MPDDKAVNGRRDFLRKTLTVIPAVTLAGYGVG	*Yersinia pestis*
PA4621	Aldehyde oxidase	Periplasmic?	MSNRDISRRAFLQGGLIAGVGVTLAPLGSQAFA	*Haemophilus influenzae*
PA1601	Aldehyde oxidase	Periplasmic?	MSLANPSRRGFLKAGGLLLVTVNLPAPLLALA	
PA1880	Aldehyde oxidase	Periplasmic?	MNSKIDLSNALPGSRRGFLKGAAVVGLTIGFQWSGARRALA	
PA2378	Aldehyde oxidase	Periplasmic?	MKRSYPDDLVIGNLSRRGFLKGVGATGVLLVAANWGWRDALA	
Others				
copA	Multicopper oxidase	Periplasmic	MHRTSRRTFVKGLAATGLLGGLGLWRAPAWA	*Caulobacter crescentus,*
PA0144	unknown	unknown	MSRSNGSSSRRTFLRLAALLLPAGALLGSLPGVRAAA	*B. parapertussis*

*The twin-arginine recognition motif (consensus RRXFLK) is underlined.
†The listed species have predicted TAT-dependent homologs based on their genome sequence; however, experimental data are not available.

were analyzed in triplicate. Under these growth conditions, *plcHR* expression is undetectable in the absence of IPTG. Pyoverdine siderophore production was detected on casamino acids agar (5 g l^{-1} casamino acids/5 mM K_2HPO_4/1 mM $MgSO_4$/1.5% agar) without or with 0.5 g l^{-1} ethylenediamine di(*o*-hydroxy)phenylacetic acid (EDDHA) after 18 h at 37°C. The anaerobic growth medium was NH_4-free M9 glucose agar containing 1% KNO_3, and GasPak Plus anaerobic jars were incubated for 48 h at 37°C. Osmotolerance was monitored in Hepes-buffered succinate medium containing NaCl and choline, and cell densities were measured after 24 h at 37°C. Carbon metabolism was assayed after 18 h of growth at 37°C on M9 agar containing 5 g l^{-1} of the individual carbon sources. Liquid M9 containing 1% *n*-hexadecane was used, and incubation was for 5 days at 32°C. Susceptibilities to growth inhibitors were determined by disk diffusion assays on a lawn of approximately 10^8 bacteria on M9 glucose agar. Motility plates to detect swimming, swarming, and twitching were prepared as described (12). Biofilms were grown statically in polypropylene tubes for 2 days at 32°C in Hepes-buffered succinate medium, after which growth was measured and the resulting biofilms were visualized by staining with crystal violet (13).

General Genetic and Biochemical Techniques. Isogenic mutant strains affected in specific genes were generated by allelic exchange of an internal gene fragment with a gentamicin-resistance cassette as described (14, 15), and gene replacements were verified by PCR across the region. For genetic complementation of the *tatC* mutant, a 4-kb *Pst*I DNA fragment containing the entire *tat* locus was cloned into mini CTX1 (16) and integrated in a single copy at the *attB* locus, yielding the complemented *tatC* mutant (*tat*$^+$). Genetic complementation of the ADΔ*tatC*/pADD-*plcHR* was achieved by plasmid pVLT-*tat,* which provided the 4-kb *tat* locus in *trans*. Site-directed mutagenesis of twin-arginine motifs was performed with a PCR-based protocol (17), and the mutated copy of the gene was provided on a plasmid in corresponding deletion mutants. β-Galactosidase activities in soluble cell extracts were determined with *o*-nitrophenyl-β-D-galactoside (ONPG) as the substrate. Pyoverdine concentrations in culture supernatants were determined by measuring the absorbance at 403 nM.

Pulmonary Animal Model. Bacteria were grown for 18 h at 32°C in low phosphate succinate medium, embedded into agarose beads, and free bacterial cells were removed as published (18). The number of organisms incorporated into the beads was determined by plating serial dilutions, and 0.1 ml of a slurry of beads in PBS was administered directly into the trachea of 8-week-old male Harlan–Sprague–Dawley rats. Six days after infection, the lungs were homogenized in PBS with a tissue tearer, and appropriate dilutions were plated to determine the colony forming units. For histopathological examination, lungs were fixed in formalin and stained with hematoxylin and eosin.

Results and Discussion

Pleiotropic Effects of a *P. aeruginosa* tat Mutation. A screening of the *P. aeruginosa* protein database (www.pseudomonas.com) based on the conserved TAT-recognition signal sequence motif RRXFLK/R (19) revealed the presence of at least 18 putative TAT-dependent secreted products (Table 1). This screening was done

manually by browsing through the entire genome containing 5,570 annotated protein sequences. The screening criteria included the presence of a twin-arginine, at least one additional conserved residue within the TAT-recognition motif, a hydrophobic core, and a possible signal sequence cleavage site (AXA). Additional TAT-dependent proteins harboring less-conserved signal sequences may likely exist. Some of the TAT-dependent proteins listed in Table 1 are extracellular, whereas others are predicted to be located in either the periplasm or in the outer membrane. A stable *tatC* deletion mutant conferred pleiotropic phenotypes compared with *P. aeruginosa* PAO1 wild type, supporting the database screening results. The influence of the TAT apparatus on several proven or putative virulence factors was studied in greater detail.

Twin-Arginine Motif and Secretion of Overexpressed Phospholipase C. Two phospholipases, PlcH and PlcN, have recently been shown to require the TAT pathway in *P. aeruginosa* PAK (10). We further studied PlcH secretion with the *P. aeruginosa* PAO1-derived T7-overexpression system ADD1976, in which the *plcHR* operon is transcribed from the IPTG-inducible T7 promoter of plasmid pADD3268 (11). Induction of *plcHR* in ADD1976 resulted in high levels of extracellular PlcH, as shown by activity on the synthetic substrate NPPC and by Western blot analysis (Fig. 1*A*). In contrast, an isogenic ADDΔ*tatC* mutant strain lacked such NPPC activity on *plcHR* induction, and PlcH was absent but was restored by providing a plasmid-borne functional *tat* locus. To show directly the involvement of TAT in the secretion of PlcH, the PlcH signal sequence was altered at the twin-arginine motif by site-directed mutagenesis (17). Overexpression of this mutated version (PlcH-R9K) in the ADD1976 wild type or in ADDΔ*tatC* yielded very low NPPC activity, and PlcH was absent in culture supernatants (Fig. 1*A*). Occasionally, a slower migrating form of PlcH-R9K, presumably unprocessed enzyme as a result of cell lysis, was detectable after longer exposure in Western blot analysis (data not shown). These findings provide direct evidence that PlcH harbors an essential TAT-dependent signal sequence and that export of PlcH occurs exclusively through the TAT secretion apparatus. PlcH has been shown to play an important role in virulence (20, 21).

Role of the TAT System in Pyoverdine-Mediated Iron Acquisition. The PAO1Δ*tatC* mutant lacked the yellow-green fluorescent pigment pyoverdine, which is a powerful siderophore essential for iron acquisition and has been associated with virulence (22). PAO1Δ*tatC* mutant cells were nonpigmented and failed to grow in the presence of the iron-chelator EDDHA (Fig. 1*B*). Unlike other mutants affected in pyoverdine biosynthesis, such as Δ*pvdD*, Δ*tatC* cells were not rescued by crossfeeding pyoverdine from PAO1 wild type (Fig. 1*B*), indicating that the Δ*tatC* mutation affects both biosynthesis and uptake of pyoverdine. This phenotype was also observed after deletion of the *tatC* gene in other strains such as PAK and PA14 (Fig. 1*B*). We identified at least two genes within the *pvd* locus that encode proteins with putative TAT-like signal sequences. PA2398 (*fpvA*) encodes the outer membrane receptor essential for binding and uptake of pyoverdine (23). The ferripyoverdine receptor has been reported to contain a long and unusual signal sequence (24), and here we demonstrate that FpvA export is in fact TAT-dependent. A mutant strain producing an FpvA protein with an altered TAT-recognition motif (*fpvA*-R18K) secreted less pyoverdine (88 μg ml^{-1}) than wild type (324 μg ml^{-1}) and failed to grow in the presence of EDDHA (Fig. 1*B*). This finding indicates that strain *fpvA*-R18K lacked a functional ferripyoverdine receptor and was therefore unable to use pyoverdine. PA2394 encodes a putative aminotransferase harboring a TAT-like signal sequence. Mutant strains carrying a deletion of PA2394 or a specific mutation affecting the TAT-recognition motif (PA2394-R5K) produced pyoverdine at reduced levels compared with wild type and were unable to grow on EDDHA-containing agar media. Thus, the protein encoded by PA2394 represents a second TAT-dependent factor involved in pyoverdine-mediated iron acquisition. However, because neither the specific mutations in *fpvA* nor in PA2394 completely abolished pyoverdine production, additional pyoverdine biosynthetic enzymes may also be TAT-dependent. Candidate genes encoding such factors are PA2392 and PA2389, both of which are essential for pyoverdine production.

Effect of TAT on Anaerobiosis and Osmotolerance. Another intriguing phenotype of *tat* mutants was related to growth under oxygen restriction. Although *P. aeruginosa* prefers aerobic respiration, it is capable of growing under anaerobic conditions in the presence of nitrogenous oxides, which can serve as terminal electron acceptors (25). This denitrification pathway to reduce nitrate to nitrogen gas is catalyzed by four reductases. The first step, the enzymatic conversion of nitrate to nitrite, involves a six-gene cluster (*napEFD-ABC*). We found that two periplasmic proteins encoded in this gene cluster, NapA, the nitrate reductase, and NapF, a ferredoxin, both contained TAT-dependent signal sequences. Mutant strains affected in *tatC* were impaired in growth under anaerobic conditions in the presence of nitrate, and an identical phenotype was caused by a mutation in *napA* (Fig. 1*C Left*). These strains were still capable of using nitrate as a sole nitrogen source during aerobic growth, indicating that the assimilatory nitrate reduction pathway (NasA) was not affected by TAT (26). Interestingly, the reductase NosZ, which converts nitrous oxide to nitrogen gas, also seems to be TAT-dependent, as recently demonstrated for *Pseudomonas stutzeri* (27). The TAT-dependent denitrification pathway may be significant in patients with cystic fibrosis (CF) infected with mucoid *P. aeruginosa*, where alginate has been shown to restrict diffusion of oxygen, thus creating a microaerobic or anaerobic environment (28), and where nitrate levels are increased (29). Also, CF airway fluid, as a consequence of the dehydrating condition, is a high osmolar environment, which impairs the epithelial cells in killing bacteria (30). *P. aeruginosa* resists high osmolarity, at least in part because of its capability to generate the osmoprotectant glycine-betaine from the lung surfactant phosphatidylcholine or choline (31). In contrast to PAO1 wild type, the Δ*tatC* mutant failed to grow in an increased osmolarity environment created by 0.5 M NaCl (Fig. 1*C Right*). Higher osmolarity generated by 0.7 M NaCl impaired growth of wild-type cells unless choline was added, and this rescue effect was abolished in Δ*tatC* mutant cells (Fig. 1*C Right*). These data provide strong evidence for a role of the TAT system in resistance to osmotic stress.

Role of the TAT System in Carbon Metabolism and Detoxification. The TAT translocation system plays an important role in the physiology of *P. aeruginosa*. In contrast to PAO1 wild-type cells, Δ*tatC* mutant cells failed to grow on media containing 0.5% choline as the sole carbon and nitrogen source (Fig. 1*D*). Additional carbon sources were tested to determine whether they would support growth of Δ*tatC* mutant cells. The mutation in the *tat* locus also had an effect on glucose utilization. In the Entner–Doudoroff pathway, glucose is degraded through the key intermediate 6-phosphogluconate to glyceraldehyde-3-phosphate and pyruvate. The initial steps in the conversion of glucose to 6-phosphogluconate are the subsequent oxidation to gluconate and 2-keto-gluconate (32). We found a TAT-dependent signal sequence in the gene product of PA2264, which encodes a putative sugar dehydrogenase and is located in a cluster of genes implied in the utilization of 2-keto-gluconate (33). Growth assays indicated that the Δ*tatC* mutant was capable of using glucose and gluconate but not 2-keto-gluconate as sole carbon source (Fig. 1*D*). Growth on succinate, glycerol, lactate, and the polyether Tween-20 was not affected in Δ*tatC* mutant cells. However, the *tat* mutation abrogated the utilization of *n*-hexadecane (Fig. 1*E*). Hydrocarbon degradation starts with three terminal oxidation steps to the corresponding alcohol, aldehyde, and acid, involving a monooxygenase, alcohol dehydrogenase, and aldehyde dehydrogenase (34). These reactions take place outside the cyto-

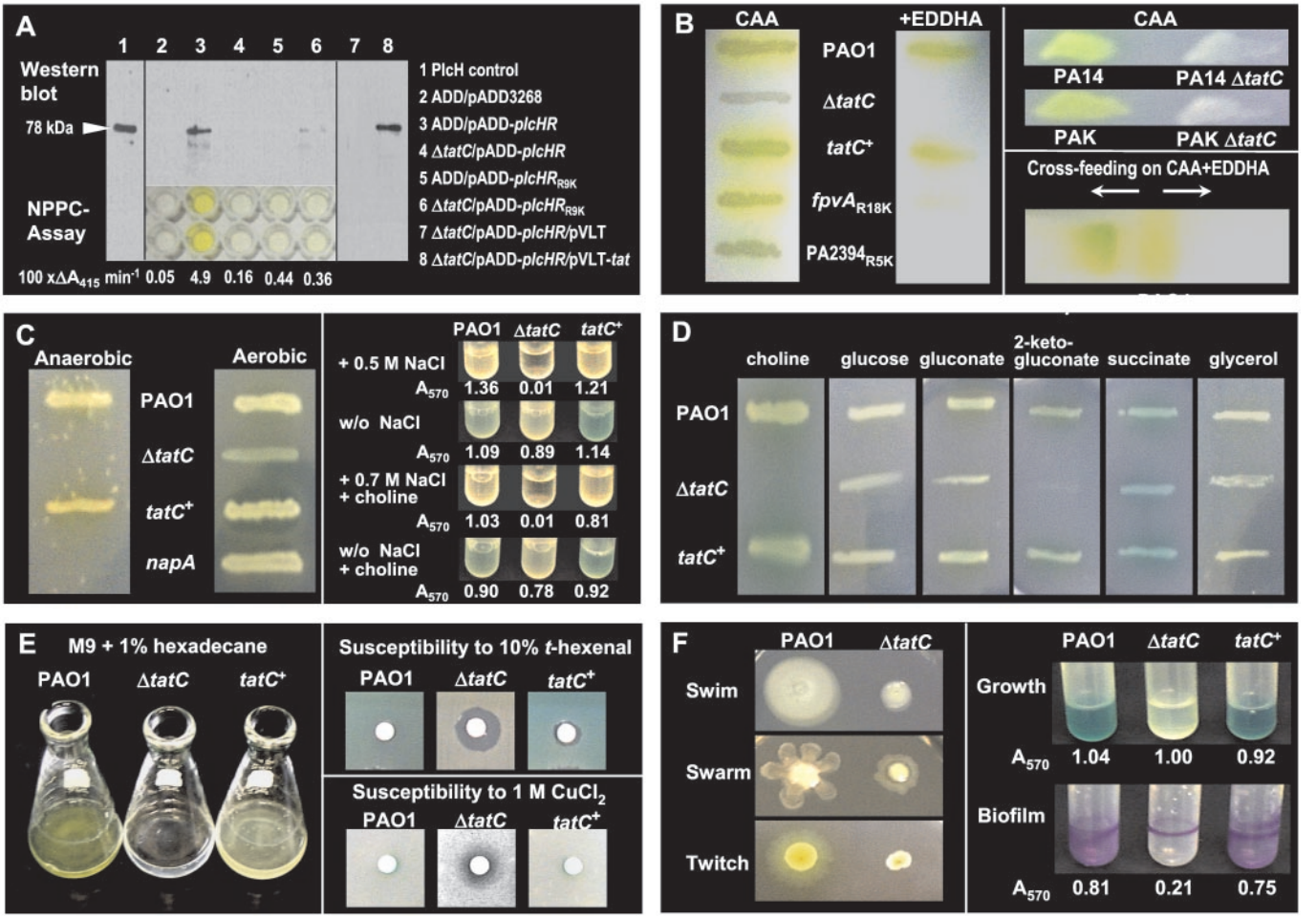

Fig. 1. Multiple phenotypes of PAO1Δ*tatC* mutant cells. (*A*) Secretion of PlcH in ADD wild type and ADDΔ*tatC* after overexpression of wild-type *plcHR* or mutated $plcHR_{R9K}$. The activity of supernatants on the synthetic substrate NPPC was measured and PlcH was detected by Western blot analysis. The 78-kDa band corresponding to mature PlcH is indicated by an arrowhead, and purified PlcH was used as control. (*B*) Production of the yellow-green siderophore pyoverdine on low iron media. Included are the phenotypes of PAO1 wild-type, Δ*tatC* mutant, complemented mutant (tat^+) and site-specific mutants affected in the TAT-recognition motif of the FpvA and PA2394 signal sequences, growth characteristics on casamino acids (CAA) agar in the presence of the iron-chelator EDDHA, and crossfeeding by pyoverdine-producing wild type. (*C*) Anaerobic growth by denitrification compared with aerobic growth on M9 agar containing 1% nitrate (*Left*). Osmotolerance to salt, with or without choline as an osmoprotectant, was assessed by measuring growth in the presence of the indicated concentrations of NaCl (*Right*). (*D*) Utilization of various carbon sources. Various compounds, including choline and 2-ketogluconate, were tested whether they support growth of Δ*tatC* cells. (*E*) Aldehyde conversion as part of hydrocarbon degradation (*Left*) and susceptibilities to the antimicrobial *t*-hexenal and copper chloride (*Right*). (*F*) Motility characteristics relating to swimming, swarming, and twitching (*Left*), and biofilm formation (*Right*).

plasm to avoid toxicity of the aldehyde intermediates. We detected at least four distinct aldehyde dehydrogenases, encoded by PA4621, PA1601, PA1880, and PA2378, with TAT-like signal sequences for export to the periplasm. The lack of aldehyde dehydrogenase activity in Δ*tatC* mutant cells would explain their inability to use hexadecane. Interestingly, Δ*tatC* mutant cells were hypersusceptible to the nonmetabolizable aldehyde *t*-hexenal (Fig. 1*E*), which is a naturally occurring antimicrobial agent found in apples (35, 36). The susceptibility of Δ*tatC* mutant cells to other compounds was investigated by disk diffusion assays, and we found increased inhibition of growth by copper chloride (Fig. 1*E*), which was presumably a result of the lack of the TAT-dependent CopA multicopper oxidase. In contrast, Δ*tatC* mutant cells and PAO1 wild-type cells exhibited identical susceptibilities to oxidative stress-generating compounds such as hydrogen peroxide and cumene hydroperoxide (data not shown).

Altered Motility and Biofilm Formation in TAT-Deficient Strains. The deletion of the *tat* locus in PAO1 had a dramatic effect on bacterial motility (Fig. 1*F*). *P. aeruginosa* is capable of three types of motility: (*i*) flagella-mediated swimming; (*ii*) swarming, characterized by elongated and hyper-flagellated cells on a thin surface fluid layer; and (*iii*) twitching, which depends on type IV pili (37, 38). The Δ*tatC* mutant failed to spread on swim agar compared with wild type, which demonstrated fast growth in concentric circles. Also, Δ*tatC* mutant cells failed to produce the typical dendritic branching growth exhibited by swarming wild-type tendrils. Twitching motility was essentially absent in Δ*tatC* mutant cells when the hazy zone of growth at the agar/Petri dish interface was measured. Interestingly, Δ*tatC* mutant cells appeared to be able to swim and twitch when examined microscopically, indicating that they possessed flagella and pili. Moreover, a subpopulation of the Δ*tatC* mutant cells, but not wild-type cells, formed filamentous aggregates consisting of 4–15 bacteria, and these aggregates were still motile. Analysis of all known genes involved in flagella and pili synthesis and assembly did not reveal any TAT-dependent products. Taken together, these data suggest that the less motile phenotype observed on agar plates is either an indirect effect of abnormal function of flagella and pili or the consequence of improper chemotaxis, or both. A similar phenotype has recently been demonstrated for *P. aeruginosa* mu-

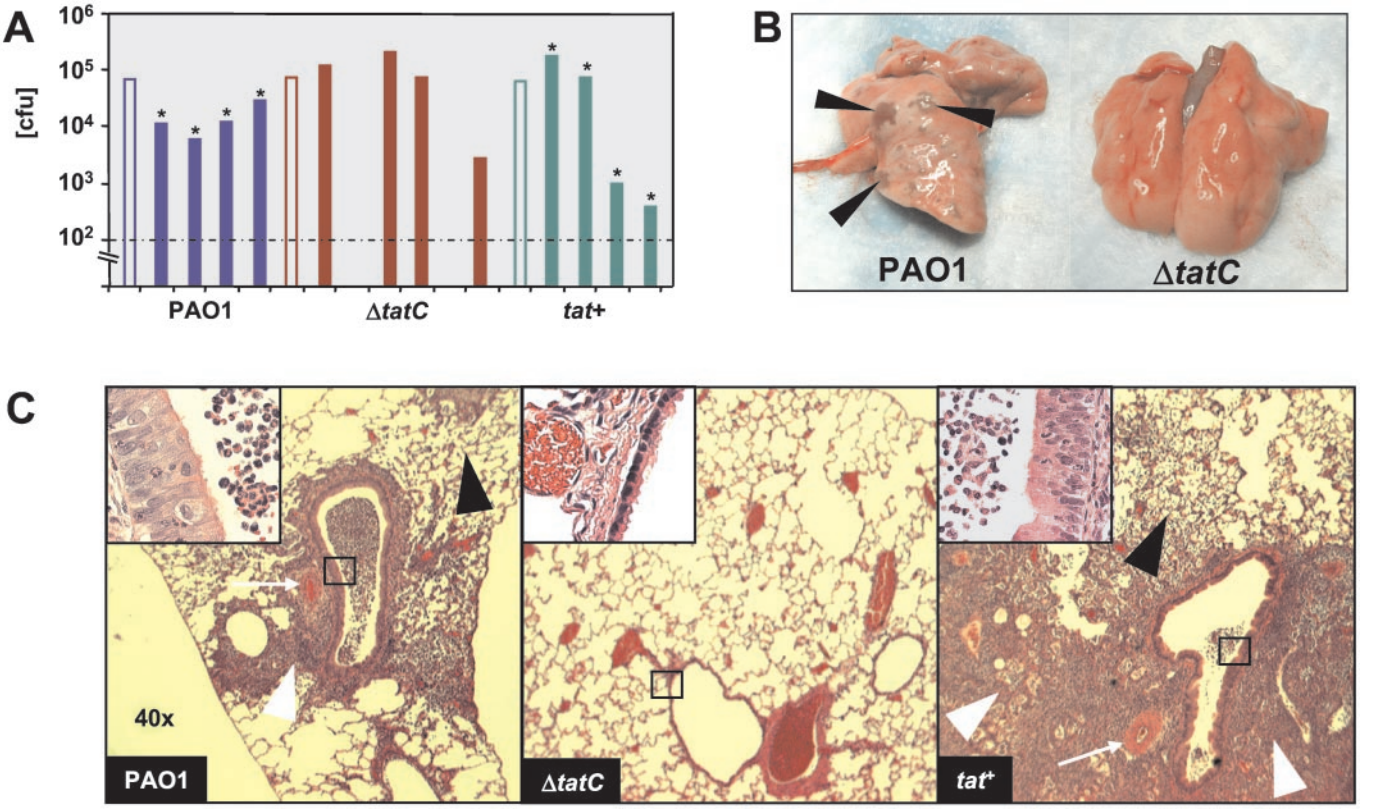

Fig. 2. Role of the TAT system in pathogenesis. (*A*) Colony-forming units retrieved from lungs 6 days after infection (solid bars) and the numbers of bacteria in the inoculum (open bars). The detection threshold is indicated by a dashed line. Individual lungs with gross lesions are marked with an asterisk. (*B*) Pulmonary abscesses were detected on rat lungs infected with PAO1 wild-type cells (arrowheads), but were not observed on lungs infected with Δ*tatC* mutant bacteria. (*C*) Histopathologic effects as a result of infection with *P. aeruginosa*. Pulmonary congestion (white arrows) and dense perivascular infiltrations of mononuclear inflammatory cells (white arrowheads) were detected, with extensions of inflammatory cells into the alveolar lumen leading to the degeneration of the pulmonary architecture (black arrowheads). *Insets* show the selected areas in a ×315 magnification and demonstrate peribronchiolar inflammation with thick, elongated epithelial cells and heavy accumulation of polymorphonuclear cells in the bronchiolar lumen.

tants affected in the *ppk* gene for polyphosphate kinase (38). Flagella-mediated motility and pili-dependent twitching are essential for the formation of biofilms (39). Consequently, it was not surprising to see an effect of the Δ*tatC* mutation on biofilm formation. Although growth of PAO1, Δ*tatC* mutant cells, and complemented mutant cells in static cultures was comparable in terms of final cell densities and homogeneity, staining of the resulting biofilms revealed a dramatic difference (Fig. 1*F Right*). All strains formed biofilms at the interface between the air and the medium. However, Δ*tatC* mutant cells had apparently not attached to the polypropylene tube beyond that interface, as observed for wild-type cells and for complemented mutant cells. This phenotype was observed in Hepes-buffered low-phosphate/succinate medium and in low iron casamino acid medium, but not in LB. Thus, environmental conditions such as nutrient availability seem to influence the effect of a *tat* deletion on biofilm formation. Whether this is because of altered motility or chemotaxis remains to be investigated. However, biofilms play an important role in pathogenesis, because they are present in the lungs of patients with chronic *P. aeruginosa* infections (40).

Indirect Effects of TAT on the Levels of Exotoxin and Protease. The Δ*tatC* mutant strain was analyzed for the production of additional virulence factors including exotoxin A and protease PrpL, which are both regulated by low iron conditions and are subject to pyoverdine signaling (41). Because we demonstrated the absence of pyoverdine in the Δ*tatC* mutant, a down-regulation of exotoxin and PrpL was predictable. In fact, we found that the transcription of the *toxA* and *prpL* genes was significantly decreased to 25% and 30% of wild-type levels (data not shown). This finding adds two additional important proteins to the list of virulence factors affected by TAT.

Attenuated Virulence of a *tatC* Mutant Strain in a Pulmonary Animal Model. The importance of the TAT system in virulence and pathogenesis was investigated in a rat lung model that mimics a chronic infection by *P. aeruginosa* (18). Bacterial cells contained within agarose beads were administered directly into the trachea of 8-week-old male Harlan–Sprague–Dawley rats. In the first experiment 10 rats per group were infected with beads containing 50,600 ± 1,200 wild-type cells or 75,000 ± 1,800 Δ*tatC* mutant cells. The rats were killed 6 days after infection and the lungs were examined. In the group of rats infected with wild-type bacteria, 7 of 10 lungs showed multiple lesions. In contrast, none of the lungs infected with Δ*tatC* mutant cells demonstrated visible lesions. Bacteria were recovered from 8 of the 10 lungs in each group, and the colony counts retrieved from the lungs in both groups were similar (data not shown). In a second experiment, three groups of seven rats were challenged with 71,000 PAO1 wild-type cells, 76,000 Δ*tatC* mutant cells, or 65,000 complemented mutant cells. The lungs were examined for lesions and colony forming units 6 days after infection (Fig. 2*A*). The bacterial load in two rats infected with the Δ*tatC* strain was below the detectable threshold, suggesting that in these cases the Δ*tatC* bacteria were unable to survive even in a microenvironment protected by agarose beads. Abscesses with focal hemorrhage were present in all lungs infected with wild-type bacteria, but were not observed in lungs infected with Δ*tatC* cells

(Fig. 2*B*), Complementation of the Δ*tatC* mutant restored the formation of lesions to the extent observed for wild-type bacteria (data not shown, and Fig. 2 *B* and *C*). Representative lungs from each group were studied in greater detail by histopathological examination (Fig. 2*C*). Most notable in lungs infected with wild-type or *tat*$^+$ bacteria were the congestion of blood vessels and the perivascular accumulation of densely packed mononuclear (macrophage-type) cells. There was extension of these inflammatory cells into adjacent alveoli. Also, intense neutrophilic peribronchial inflammation was present, and many polymorphonuclear inflammatory cells were detected in the bronchiolar lumen. In contrast, lungs infected with Δ*tatC* mutant cells seemed intact and essentially devoid of inflammation.

Conclusions

We have shown that the TAT apparatus affects multiple proteins located in the periplasm, outer membrane, or extracellular milieu. Experimental evidence has been provided for the direct involvement of the TAT system in the secretion of many factors with an undisputed role in bacterial virulence, including phospholipases and proteins required for pyoverdine-mediated iron uptake, anaerobic respiration, and choline degradation. Additional traits linked to virulence, such as osmotolerance, motility, and biofilm formation, may be indirectly affected by TAT and the molecular genetic mechanisms leading to the phenotypes observed in *tat* mutants need to be elucidated in greater detail. A mutation in the *tat* locus abrogated the destructive pathological effects of *P. aeruginosa* on lung tissue in a rat model of chronic infection. A brief screening of microbial genome sequences indicates that the TAT apparatus is well conserved among bacterial pathogens, including *Mycobacterium tuberculosis*, *Staphylococcus aureus*, and *Helicobacter pylori*. Interestingly, the phospholipase C homologs of *M. tuberculosis* possess conserved TAT-dependent signal peptides. The TAT system is absent in higher eukaryotes, thus, it represents a potential target for development of novel antimicrobial agents. Because the TAT apparatus is located in the cytoplasmic membrane, a putative drug may be active in the periplasm. This would circumvent many problems related to drug delivery to the cytoplasm, including induction of efflux pumps (42). Several reports indicate some specificity of TAT for cognate substrates (43), therefore it may be possible to design inhibitors with a broad host range as well as antimicrobial agents specific for single pathogens that would not affect the normal flora.

We thank Patricia Skavlen for technical assistance in histopathological diagnosis. This work was funded by grants from the National Institutes of Health (AI-15940), from the Heart, Lung, and Blood Institute (HL-62608), and from the Cystic Fibrosis Foundation (to M.L.V.).

1. Driessen, A. J., Fekkes, P. & van der Wolk, J. P. (1998) *Curr. Opin. Microbiol.* **1,** 216–222.
2. Sandkvist, M. (2001) *Mol. Microbiol.* **40,** 271–283.
3. Kaufman, M. R. & Taylor, R. K. (1994) *Methods Enzymol.* **235,** 426–448.
4. Robinson, C. & Bolhuis, A. (2001) *Nat. Rev. Mol. Cell. Biol.* **2,** 350–356.
5. Berks, B. C., Sargent, F. & Palmer, T. (2000) *Mol. Microbiol.* **35,** 260–274.
6. Chaddock, A. M., Mant, A., Karnauchov, I., Brink, S., Herrmann, R. G., Klosgen, R. B. & Robinson, C. (1995) *EMBO J.* **14,** 2715–2722.
7. Settles, A. M., Yonetani, A., Baron, A., Bush, D. R., Cline, K. & Martienssen, R. (1997) *Science* **278,** 1467–1470.
8. Stanley, N. R., Findlay, K., Berks, B. C. & Palmer, T. (2001) *J. Bacteriol.* **183,** 139–144.
9. Berks, B. C. (1996) *Mol. Microbiol.* **22,** 393–404.
10. Voulhoux, R., Ball, G., Ize, B., Vasil, M. L., Lazdunski, A., Wu, L. F. & Filloux, A. (2001) *EMBO J.* **20,** 6735–6741.
11. Cota-Gomez, A., Vasil, A. I., Kadurugamuwa, J., Beveridge, T. J., Schweizer, H. P. & Vasil, M. L. (1997) *Infect. Immun.* **65,** 2904–2913.
12. Deziel, E., Comeau, Y. & Villemur, R. (2001) *J. Bacteriol.* **183,** 1195–1204.
13. O'Toole, G. A., Pratt, L. A., Watnick, P. I., Newman, D. K., Weaver, V. B. & Kolter, R. (1999) *Methods Enzymol.* **310,** 91–109.
14. Hoang, T. T., Karkhoff-Schweizer, R. R., Kutchma, A. J. & Schweizer, H. P. (1998) *Gene* **212,** 77–86.
15. Schweizer, H. P. & Hoang, T. T. (1995) *Gene* **158,** 15–22.
16. Hoang, T. T., Kutchma, A. J., Becher, A. & Schweizer, H. P. (2000) *Plasmid* **43,** 59–72.
17. Turner, P. C., McLennan, A. G., Bates, A. D. & White, M. R. H. (1998) *Molecular Biology* (Springer, New York).
18. Cash, H. A., Woods, D. E., McCullough, B., Johanson, W. G., Jr., & Bass, J. A. (1979) *Am. Rev. Respir. Dis.* **119,** 453–459.
19. Buchanan, G., Sargent, F., Berks, B. C. & Palmer, T. (2001) *Arch. Microbiol.* **177,** 107–112.
20. Ostroff, R. M., Wretlind, B. & Vasil, M. L. (1989) *Infect. Immun.* **57,** 1369–1373.
21. Terada, L. S., Johansen, K. A., Nowbar, S., Vasil, A. I. & Vasil, M. L. (1999) *Infect. Immun.* **67,** 2371–2376.
22. Meyer, J. M., Neely, A., Stintzi, A., Georges, C. & Holder, I. A. (1996) *Infect. Immun.* **64,** 518–523.
23. Folschweiller, N., Schalk, I. J., Celia, H., Kieffer, B., Abdallah, M. A. & Pattus, F. (2000) *Mol. Membr. Biol.* **17,** 123–133.
24. Poole, K., Neshat, S., Krebes, K. & Heinrichs, D. E. (1993) *J. Bacteriol.* **175,** 4597–4604.
25. Davies, K. J., Lloyd, D. & Boddy, L. (1989) *J. Gen. Microbiol.* **135,** 2445–2451.
26. Richardson, D. J., Berks, B. C., Russell, D. A., Spiro, S. & Taylor, C. J. (2001) *Cell. Mol. Life Sci.* **58,** 165–178.
27. Heikkila, M. P., Honisch, U., Wunsch, P. & Zumft, W. G. (2001) *J. Bacteriol.* **183,** 1663–1671.
28. Hassett, D. J. (1996) *J. Bacteriol.* **178,** 7322–7325.
29. Jones, K. L., Hegab, A. H., Hillman, B. C., Simpson, K. L., Jinkins, P. A., Grisham, M. B., Owens, M. W., Sato, E. & Robbins, R. A. (2000) *Pediatr. Pulmonol.* **30,** 79–85.
30. Smith, J. J., Travis, S. M., Greenberg, E. P. & Welsh, M. J. (1996) *Cell* **85,** 229–236.
31. Sage, A. E., Vasil, A. I. & Vasil, M. L. (1997) *Mol. Microbiol.* **23,** 43–56.
32. Lessie, T. G. & Phibbs, P. V., Jr. (1984) *Annu. Rev. Microbiol.* **38,** 359–388.
33. Swanson, B. L., Hager, P., Phibbs, P., Jr., Ochsner, U., Vasil, M. L. & Hamood, A. N. (2000) *Mol. Microbiol.* **37,** 561–573.
34. Watkinson, R. J. & Morgan, P. (1990) *Biodegradation* **1,** 79–92.
35. Corbo, M. R., Lanciotti, R., Gardini, F., Sinigaglia, M. & Guerzoni, M. E. (2000) *J. Agric. Food Chem.* **48,** 2401–2408.
36. Gardini, F., Lanciotti, R. & Guerzoni, M. E. (2001) *Lett. Appl. Microbiol.* **33,** 50–55.
37. Wall, D. & Kaiser, D. (1999) *Mol. Microbiol.* **32,** 1–10.
38. Rashid, M. H. & Kornberg, A. (2000) *Proc. Natl. Acad. Sci. USA* **97,** 4885–4890.
39. O'Toole, G. A. & Kolter, R. (1998) *Mol. Microbiol.* **30,** 295–304.
40. Hoiby, N., Krogh Johansen, H., Moser, C., Song, Z., Ciofu, O. & Kharazmi, A. (2001) *Microbes Infect.* **3,** 23–35.
41. Lamont, I. L., Beare, P. A., Ochsner, U. A., Vasil, A. I. & Vasil, M. L. (2002) *Proc. Natl. Acad. Sci. USA* **99,** 7072–7077.
42. Schweizer, H. P. (1998) *Antimicrob. Agents Chemother.* **42,** 394–398.
43. Jongbloed, J. D., Martin, U., Antelmann, H., Hecker, M., Tjalsma, H., Venema, G., Bron, S., van Dijl, J. M. & Muller, J. (2000) *J. Biol. Chem.* **275,** 41350–41357.